29th International Cosmic Ray Conference Pune (2005) **00**, 101–104

A method to measure the energy spectra of the primary heavy components at the knee using a new Tibet AS core detector array YAC

J.Huang[a], M. Shibata[b], Y. Katayose[b], L.K. Ding[c], M. Ohnishi[a], N. Hotta[d], H.B. Hu[c], T. Saito[e], M. Takita[a], and T. Yuda[f]

(a) Institute for Cosmic Ray Research, the University of Tokyo, Kashiwa 277-8582, Japan
(b) Faculty of Engineering, Yokohama National University, Yokohama 240-8501, Japan
(c) Key Lab. of Particle Astrophys., Institute of High Energy Physics, Chinese Academy of Sciences, Beijing 100049, China
(d) Faculty of Education, Utsunomiya University, Utsunomiya 321-8505, Japan
(e) Tokyo Metropolitan College of Aeronautical Engineering, Tokyo 116-0003, Japan
(f) Faculty of Engineering, Kanagawa University, Yokohama 221-8686, Japan
Presenter: J. Huang (huang@icrr.u-tokyo.ac.jp), jap-huang-J-abs2-he12-poster

The first phase experiment of the Tibet hybrid air shower core observation to measure the energy spectrum of the light components (proton and helium) strongly suggested that the knee region is dominated by heavy components. A new type of air shower core detector YAC (Yangbajing Air shower Core detector) is under the development where the capability of the explicit measurement of the heavy components are investigated. We have examined the performance of the planned apparatus and its expected sensitivity to the primary cosmic-ray composition. This new burst detector array may consist of 400 burst detectors of 0.20 m^2 placed in a grid with 3.75 m interval. Each burst detector consists of lead plates of the total thickness 3.5 cm above the scintillator attached with the photomultipliers. The Monte Carlo simulation shows that the new burst detector array is powerful enough to study the chemical composition, and in particular, to obtain the energy spectrum of the major component at the knee.

1. Introduction

The energy spectrum of observed cosmic rays is expressed by a power law from about 10^{10} to 10^{20} eV with a slight change of slopes between 10^{15} to 10^{16} eV. The break of the all particle spectrum at around several times 10^{15} eV is called the "knee". The chemical composition of the cosmic rays at the knee is considered as a key information to understand the cosmic-ray acceleration and the propagation in the galaxy [1]. The first phase of the Tibet hybrid experiment to measure the energy spectrum of the light components (proton and helium) strongly suggested that the knee region is dominated by heavy components. Thus, a new type of air shower core detector YAC (Yangbajing Air shower Core detector) is under the development where the capability of the explicit measurement of the heavy components are investigated. The merit in doing the hybrid experiment in Tibet is that the atmospheric depth of the experimental site (4300 m a.s.l., 606 g/cm^2) is close to the maximum development of the air showers with energies around the knee almost independent of the masses of primary cosmic rays. We can determine the primary cosmic-ray energy much less dependently upon the chemical composition than those experiments at the sea level [2]. Thus, the Tibet hybrid experiment enables us to measure the primary proton, helium and iron differential energy spectra by selecting them event by event.

2. Design study of the AS core detector

The design study of the new AS core detector has been made under the following requirements. (1) The energy flow characteristic of the air shower core can be measured for all kind of the primary particles, namely from protons to irons, with high detection efficiency. (2) The effective area is large enough to study the knee by given number of detectors. (3) The separation of the primary mass groups is possible with a high purity. Above mentioned requirements have been appreciated by a collection power C_p defined as

$$C_p = \eta \times P_0 \times P_1 \times D^2,$$

where η, P_0, P_1 and D denote detection efficiency, selection rate of the given primary mass group, selection rate of other primary mass groups and the distance between the detectors. The detection efficiency is also a function of the thickness of the lead plate above the scintillator. We optimized those parameters as follows. (i) Thickness of the lead is 3.5 cm. (ii) Distance between detectors is 3.75 m. (iii) Trigger condition is set as the burst size $N_b \geq 100$, the number of hit detectors $N_D \geq 5$ and the detector unit with N_b^{top} is located at inner area of BD grid excluding the most outer edges, where N_b^{top} is the maximum burst size among fired detectors. The last condition (iii) enables us to analyze the lateral spread of the energy flow at the air shower core with low burst size threshold, which is needed to detect events induced by heavy primaries. Thus, YAC array may consist of 400 burst detectors of 0.20 m^2 each. The hardware of YAC is described in [3].

3. Simulation and Analysis

A Monte Carlo (MC) simulation has been carried out on the development of air showers in the atmosphere and the response in the burst detector. The simulation code CORSIKA (version 6.200) including QGSJET01c and SIBYLL2.1 hadronic interaction models [4] are used to generate air shower events and the code EPICS [5] to generate electromagnetic cascade showers in the burst detector. Since the previous results [6, 7] are compatible with the heavily enriched primary composition at the knee, only the heavy-nuclei dominant (HD) [6] composition model is adopted as input primary in this research. The simulated data were analyzed in the same manner as in the procedure for the experimental data analysis. The detector performance, the trigger efficiency of detectors and the effective area are adequately taken into account based on the experimental conditions. The generation efficiency of the burst events by iron primary is shown in Fig. 1 as a function of the primary energy, where the difference between two interaction models are not remarkable. The ratio of the efficiency by SIBYLL to that of QGSJET model is plotted in Fig. 2, which shows less than $\sim$8% deviation from unity without any serious energy dependence. We also examined the generation efficiency of the burst events by proton and helium primaries, obtaining similar model dependence as in the case of iron primary. This model dependence was also known in previous work in analyzing the γ-families but with 30% level. The reason of the smaller dependence in YAC detector can be attributed to the lower threshold of the burst size compared with the emulsion chambers. The difference of the interaction model becomes smaller when the observed range of the secondary energy spectrum is wider. Thus, one can expect that the derivation of the primary flux for each components does not depend seriously to the interaction models used in the analysis.

The selection of the events induced by protons, heliums and irons are made with use of a feed-forward artificial

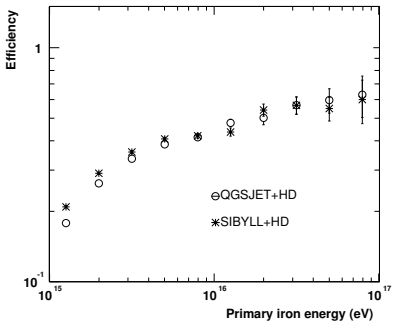

Figure 1. Generation efficiency of the burst events by iron nuclei.

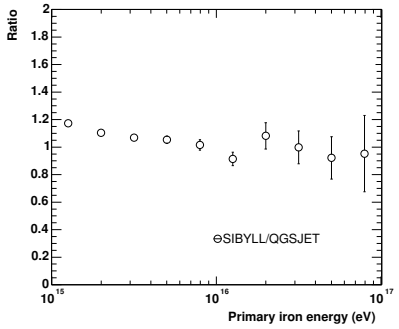

Figure 2. Relative ratio of the generation efficiency of SIBYLL to QGSJET model by iron nuclei.

neural network (ANN [8]) whose applicability to our experiment was well confirmed by the Monte Carlo simulation [6]. The trigger conditions of (1) $N_b \geq 100$, (2) $N_D \geq 5$ are applied to select 'burst events'. We have divided the MC data into two datasets. Due to the difference of the detection efficiency, air showers of the size $N_e \geq 10^5$ are enriched with 'proton+helium' origin (called tagged-I dataset), namely, the heavy-primary-induced events can hardly generate burst events in lower air shower size range, while those of $N_e \geq 10^6$ contain events of heavy-primary origin with higher detection efficiency (called tagged-II dataset). Then, we obtained 1.21×10^5 and 1.46×10^5 events for the tagged-I and tagged-II datasets, respectively, in the case of QGSJET model, while 1.37×10^4 and 1.52×10^4, in SIBYLL model. The following eleven parameters are input to the ANN with fifty hidden nodes and one output unit: (1) the number of hit detectors N_D, (2) the sum of the burst size $\sum N_b$, (3) the maximum burst size N_b^{top}, (4) the air shower size N_e, (5) age of the air shower, (6) incident zenith angle, (7) the mean lateral spread $< R >= \sum r_i/N_D$, (8) the mean energy-flow spread $< BR >= \sum N_{bi} r_i/N_D$, where N_{bi} and r_i are the burst size in each fired burst detector unit and the lateral distance from a fired detector unit to the air shower core, respectively, (9) $\frac{\sum N_b}{N_e}$, (10) $\frac{N_D}{\sum N_b}$, (11) $\frac{N_b^{top}}{\sum N_b}$. The ANN output value T is used to separate the primary groups. Those events with $T < T_c$ are treated as the candidates of lighter element group while $T > T_c$ as the heavier one, where T_c denotes a given critical target value. The values of T_c, purity (p) and the selection rate (ε) of the events satisfying the criterion are summarized in Table 1. The numbers of protons, heliums and irons thus selected agree each other within 20% between two interaction models.

Table 1. Purity(p)(%) and selection rate (ε) (%) of the selected primary groups.

E_0 (eV)		$10^{14}-10^{15}$				$10^{15}-10^{16}$				$10^{16}-10^{17}$			
	T_c\Mod	QGS		SIB		QGS		SIB		QGS		SIB	
		p	ε	p	ε	p	ε	p	ε	p	ε	p	ε
P	0.15	86.4	33.8	84.9	28.3	80.6	16.5	76.3	12.7				
P+He	0.1	96.0	51.0	95.2	46.1	91.7	32.4	91.2	30.8				
Fe	0.8					83.3	43.9	85.4	45.9	84.2	42.3	89.0	48.2

4. Results and Discussion

In Fig. 3, we show the estimated iron energy spectra using tagged-II dataset compared with the assumed one. As seen in this figure, the input spectrum is well reproduced above 2 PeV by above mentioned procedures within statistical errors in both interaction models. We can also analyze the energy spectra of the light components from the tagged-I dataset, as shown in Fig. 4 (proton) and Fig. 5 (helium), where the helium spectra are obtained by subtracting the proton spectra from the 'proton+helium' spectra.

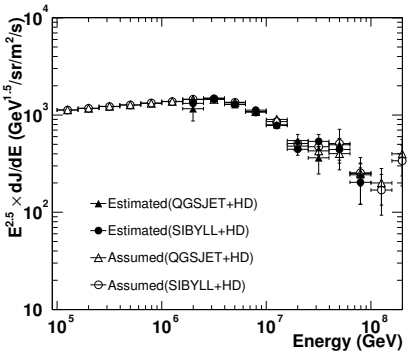

Figure 3. Energy spectra of primary iron nuclei.

Present work shows that the YAC array enables us to measure the primary proton, helium and iron differential energy spectra at the knee. The method of the analysis is based on the air shower simulation and the neural

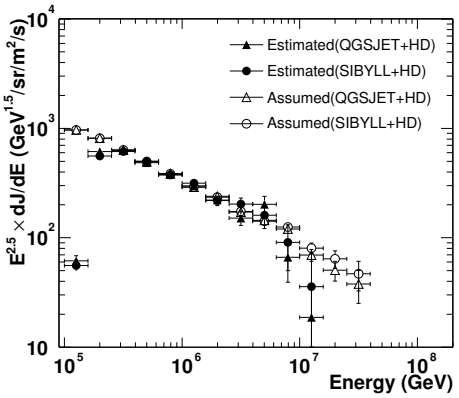

Figure 4. Energy spectra of primary protons.

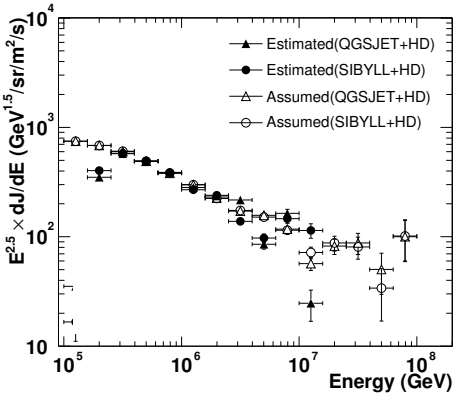

Figure 5. Energy spectra of Helium nuclei.

network, where the interaction model dependence was carefully examined and it is estimated to be at $\sim$20% level in deriving the primary flux of the given component.

5. Acknowledgements

The authors would like to express their thanks to the members of the Tibet ASγ collaboration for the fruitful discussions. The support of the JSPS (J.H., grant No. P03025) is also acknowledged.

References

[1] P.O. Lagage et al., Astron. Astrophys. 118, 223 (1983).
[2] M. Amenomori et al., ApJ. 461, 408 (1996).
[3] Y.Katayose et al., ICRC29 (2005) HE 1.5
[4] D. Heck, et al., Report **FZKA 6019**, 1998 ; http://www-ik3.fzk.de/ ~heck/corsika/physics_description/corsika_phys.html.
[5] K. Kasahara, et al., http://eweb.b6.kanagawa-u.ac.jp/~kasahara/ResearchHome /EPIC-SHome/index.html.
[6] M. Amenomori et al., Phys. Rev. D 62, 112002 (2000).
[7] M. Amenomori et al., Advances in Space Research 2004 (COSPAR) (2004).
[8] L. Lonnblad, et al., Comp. Phys. Com. 81, 185 (1994).